

# Extracellular K<sup>+</sup> Activity Changes Related to Electroretinogram Components

## *I. Amphibian (I-Type) Retinas*

EVAN DICK and ROBERT F. MILLER

From the Departments of Ophthalmology, Physiology and Biophysics, Washington University School of Medicine, St. Louis, Missouri 63110

**ABSTRACT** Electroretinographic (ERG) and extracellular potassium activity measurements were carried out in superfused eyecup preparations of several amphibians. Light-evoked changes in extracellular K<sup>+</sup> activity were characterized on the bases of depth profile analysis and latency measurements and through the application of pharmacological agents that have selective actions on the retinal network. Three different extracellular potassium modulations evoked at light onset were identified and characterized according to their phenomenological and pharmacological properties. These modulations include two separable sources of light-evoked increases in extracellular K<sup>+</sup>: (*a*) a proximal source that is largely post-bipolar in origin, and (*b*) a distal source that is primarily or exclusively of depolarizing bipolar cell origin. The pharmacological properties of the distal extracellular potassium increase closely parallel those of the b-wave. A distal light-evoked decrease in extracellular potassium appears to be associated with the slow PIII potential, based on a combination of simultaneous intracellular Müller cell recordings and extracellular ERG and potassium activity measurements before and during pharmacological isolation of the photoreceptor responses. The extracellular potassium activity increases are discussed with respect to the Müller cell theory of b-wave generation.

### INTRODUCTION

The vertebrate electroretinogram (ERG) has been analyzed extensively using various techniques designed to associate individual ERG components with activities of specific groups of retinal neurons. Particular success has been achieved in associating the a-wave with photoreceptor activity (Penn and Hagins, 1969; Hagins et al., 1970) and the corneal-positive component of the c-wave with light-evoked changes in transmembrane polarization of the retinal pigment epithelium (RPE) (Noell, 1951, 1953; Steinberg et al., 1970, 1980; Steinberg, 1971; Schmidt and Steinberg, 1971; Steinberg and Miller, 1973; Oakley, 1975, 1977; Oakley and Green, 1976; Vogel, 1980). Several hypotheses suggest that certain ERG

Address reprint requests to Dr. Evan Dick, Health Care Division, Monsanto Company, 800 N. Lindbergh Blvd., St. Louis, MO 63167.

components are generated by passive,  $K^+$ -mediated currents through Müller cells, the primary glial element in retina. Presumably, these currents are initiated by extracellular  $K^+$  activity ( $K_o^+$ ) fluctuations associated with neuronal activity. Particularly important is the hypothesis that a light-evoked  $K_o^+$  increase initiates the b-wave (Faber, 1969; Miller and Dowling, 1970*a, b*). Slow PIII is also thought to be initiated, as is the RPE component of the c-wave, by a light-evoked  $K_o^+$  decrease that results primarily from a change in the rod transmembrane potential (Faber, 1969; Zuckerman, 1973; Witkovsky et al., 1975; Oakley, 1977; Karwoski and Proenza, 1978; Lurie and Marmor, 1980). However, in contrast to the corneal-positive RPE component of c-wave, slow PIII, the corneal-negative, retinal component of c-wave, is generated, presumably by Müller cells.

To further evaluate the neuronal activities that underlie the b-wave and slow PIII, we have studied light-evoked  $K_o^+$  modulations using extracellular voltage and  $K^+$ -selective microelectrode techniques in superfused and freshly excised eyecup preparations of mudpuppy, toad, and tiger salamander, and in the isolated, superfused rabbit retina eyecup preparation. The findings reported here include an analysis in amphibian (I-type; Granit, 1935) retinas of three principal  $K_o^+$  modulations that occur at light onset, which we have identified and characterized on the basis of phenomenological and pharmacological properties. The use of pharmacological agents has made it possible to selectively isolate particular  $K_o^+$  modulations and correlate them with specific neuronal activities and electroretinographic events. In the following paper (Dick et al., 1985), we will present a similar analysis in the rabbit (E-type) retina. Preliminary results of this work have been presented elsewhere (Dick and Miller, 1977, 1978*b*; Dick et al., 1979).

## METHODS

### *Preparation, Light Stimulation, and Intracellular Recordings*

The superfused amphibian eyecup preparation, light stimulation techniques, and intracellular recording methods used in the present study were those previously reported in detail by Miller and Dacheux (1976). Experimental animals used in the present study included mudpuppies (*Necturus maculosus*), toads (*Bufo marinus*), and tiger salamanders (*Ambystoma tigrinum*). ERGs reported in this study are intraretinal ERGs, which represent the potentials recorded between an Ag/AgCl ground reference electrode located behind the eyecup and a Ringer's-filled micropipette advanced into the retina.

The control perfusate used for most of these experiments was a bicarbonate-buffered amphibian Ringer's solution composed of (mM): 86.0 NaCl, 3.0 KCl, 1.8 CaCl<sub>2</sub>, 1.0 MgCl<sub>2</sub>, 25.0 NaHCO<sub>3</sub>, 0.8 Na<sub>2</sub>HPO<sub>4</sub>, 1.0 NaH<sub>2</sub>PO<sub>4</sub>, and 10.0 glucose. A pH of 7.8 was maintained by constant aeration of the perfusates with a 98% O<sub>2</sub>/2% CO<sub>2</sub> gas mixture. For experiments where Co<sup>++</sup> was used to block chemically mediated synaptic transmission, a HEPES- (*N*-2-hydroxyethylpiperazine-*N'*-2-ethanesulfonic acid) buffered Ringer's was used to prevent precipitation of CoCO<sub>3</sub>. The HEPES-buffered Ringer's solution was composed of (mM): 111 NaCl, 3 KCl, 1.8 CaCl<sub>2</sub>, 1.0 MgCl<sub>2</sub>, 0.8 Na<sub>2</sub>HPO<sub>4</sub>, 1.0 NaH<sub>2</sub>PO<sub>4</sub>, 3.0 HEPES, and 10.0 glucose. If necessary, a pH correction to a value of 7.8 was obtained by titration with NaOH. Experimental solutions were made by the addition of one or more pharmacological agents into a control Ringer's solution. The pharmacological agents used included: CoCl<sub>2</sub> (J.T. Baker Chemical Co., Phillipsburg, NJ),  $\gamma$ -aminobutyric acid

(Sigma Chemical Co., St. Louis, MO), and  $\alpha$ -aminopimelic acid (Sigma Chemical Co.). After the addition of a pharmacological agent(s), the pH of the experimental perfusate was checked and, if necessary, retitrated to a value of 7.8 with NaOH.

#### *K<sup>+</sup>-selective Microelectrodes*

Double-barreled K<sup>+</sup>-selective microelectrodes consisting of one K<sup>+</sup>-selective barrel and one Ringer's-filled voltage-recording barrel were fabricated by a previously described (Dick, 1979) modification of the technique of Walker (1971). The K<sup>+</sup> ion-exchanger was used in this study was Corning 477317 (Corning Medical and Scientific, Medfield, MA). Microelectrode tips were beveled on a rotating, Ringer's-moistened, 0.3- $\mu$ M grinding disk (3M Co., St. Paul, MN) with both barrels aligned parallel to the plane of the grinding disk until openings of 1–3  $\mu$ m across the beveled face were produced. Resistances of the reference barrels ranged from 30 to 70 M $\Omega$ .

Each K<sup>+</sup>-selective microelectrode was calibrated in a series of five to nine test solutions with K<sup>+</sup> activities ranging from 1 to 50 meq/liter in the presence of 120 mM NaCl. In order to derive K<sup>+</sup> activities from K<sup>+</sup> concentrations, the activity coefficient for monovalent cations in mixed aqueous electrolyte solutions was drawn from a modification of the Davies equation (Martin et al., 1969). For K<sup>+</sup> concentrations in the range of 1–10 mM, the total ionic strength of the test solutions, which actually varied from 0.121 to 0.130, was taken as 0.125, which yields a K<sup>+</sup> activity coefficient of 0.77 ( $\pm 7\%$ ). That coefficient was used both for purposes of computing the K<sup>+</sup> activities of dilute KCl solutions and in the conversion of K<sup>+</sup> electrode responses (changes in the differential voltage recorded between the reference and K<sup>+</sup>-selective barrels) to K<sup>+</sup> activity changes. In the latter case, we used the simplifying assumption that the total ionic strength of the interstitial fluid is, essentially, equivalent to that of a 125 mM NaCl solution. The K<sup>+</sup>-selective microelectrodes used in this study showed nearly log-linear potential changes of 53–55 mV/decade (a factor of 10 change in external K<sup>+</sup> activity) for external K<sup>+</sup> activities in the range of 5–50 meq/liter in the presence of 120 mM NaCl. The slope of the K<sup>+</sup>-selective electrode response per unit change in external K<sup>+</sup> activity becomes significantly reduced for K<sup>+</sup> activities in the range of 1–5 meq/liter. Since the physiological range of K<sub>o</sub><sup>+</sup> in amphibian retina is ~2–6 meq/liter, it is necessary to assign a value for the potential change developed by a K<sup>+</sup>-selective electrode per decade change in external K<sup>+</sup> (hereafter called the response slope) within this lower range of K<sup>+</sup> activities in order to be able to calculate intraretinally measured K<sub>o</sub><sup>+</sup> modulations from K<sup>+</sup>-selective electrode responses.

The response slope of a K<sup>+</sup>-selective electrode for external K<sup>+</sup> activities in the range of 2–5 meq/liter in the presence of 120 mM NaCl (92.4 meq/liter NaCl) was obtained by: (a) plotting electrode potential vs. log K<sup>+</sup> activity for all calibration solutions used; (b) fitting (by eye) a straight line between the calibration points from 2 to 5 meq/liter of K<sup>+</sup> (either three or four points were used); and (c) extrapolating, from the slope of the resulting line in b, a response slope for the K<sup>+</sup> electrode over this lower range of external K<sup>+</sup> activities. Typical K<sup>+</sup> electrode response slopes for external K<sup>+</sup> activities of 2–5 meq/liter over a fixed NaCl background were 29–33 mV/decade. These response slope values were then used to calculate K<sub>o</sub><sup>+</sup> changes from K<sup>+</sup> electrode responses according to the following formula:

$$(V_b - V_a) = R_{2-5} \log \left\{ \frac{(K_o^+)_a + [(K_o^+)_b - (K_o^+)_a]}{(K_o^+)_a} \right\},$$

where  $V_a$  is the K<sup>+</sup> electrode potential at a given point  $a$  in the electrode response;  $V_b$  is the K<sup>+</sup> electrode potential at a given point  $b$  in the electrode response;  $R_{2-5}$  is the response slope (in millivolts per decade change in external K<sup>+</sup>) of the K<sup>+</sup> electrode for the K<sup>+</sup>

activities of 2–5 meq/liter in the presence of 120 mM NaCl;  $(K_o^+)_a$  is the extracellular  $K^+$  activity (in milliequivalents per liter) at point *a*; and  $(K_o^+)_b$  is the extracellular  $K^+$  activity (in milliequivalents per liter) at point *b*.

### Recordings

During this study, two preamplifiers were used for measuring the potentials from  $K^+$ -selective microelectrodes. The first amplifier used did not possess capacitance neutralization capabilities. The output of the  $K^+$ -selective microelectrode barrel was led into the noninverting side of an instrumentation amplifier (4253, Teledyne-Philbrick, Dedham, MA). The output of the reference barrel was led simultaneously to the inverting side of the T-P 4253 and the noninverting side of a T-P 1023 FET operational amplifier. The preamplifier output from each channel was led through: (*a*) an instrumentation amplifier (T-P 4253) for additional gain and DC offset control; (*b*) a low-pass filter (Brown et al., 1973, p. 394) with a high-frequency cut-off of 100 Hz; and (*c*) an active 60-Hz notch filter (783R3Q10, Frequency Devices, Haverhill, MA). The signals were then fed to one channel of a Tektronix R5103N storage oscilloscope (Tektronix Inc., Beaverton, OR) and one channel of a penwriter. Figure illustrations were photographically reproduced from penwriter records or Polaroid photographs of the storage oscilloscope display.

A second preamplifier that had both direct- and cross-capacitance neutralization capabilities was fabricated for this study. A schematic of this amplifier is shown in Fig. 1A. The input stages for the  $K^+$ -selective and reference barrels are 42J FET operational amplifiers (Analog Devices, Inc., Norwood, MA). Zero-capacitance, direct-capacitance, or cross-capacitance neutralization could be switched in as desired. At the outset of an experiment, a double-barreled  $K^+$ -selective microelectrode was positioned in an eyecup preparation and the amount of positive feedback current was adjusted for each electrode in order to: (*a*) maximally increase the rise time of the reference channel to a 400-mV, 120-Hz square wave applied to the Ag/AgCl electrode behind the eyecup preparation, and (*b*) maximally reduce, in the ion output channel, the capacitive "cross-talk" transients associated with the test potential. By removing all filtering devices and switching between zero and maximally adjusted direct- or cross-capacitance neutralization, the response characteristics of the electrode preamplifier system could be compared in these three states. A comparison of this type, but carried out in a simple Ringer's bath, is illustrated in Fig. 1B. Fig. 1B (left) shows that without employing capacitance neutralization, the differential output from the  $K^+$  electrode channel contains electrical cross-talk artifacts. These artifacts result from recording differentially between two electrodes that had very different time constants and were capacitively coupled. The time constant of the  $K^+$  barrel is much longer than that of the reference barrel and this, coupled with the frequency of the test potential (120 Hz), results in the  $K^+$  electrode itself contributing very little to the voltages recorded in the middle traces of Fig. 1B (left). The largest and most rapid rising components of the cross-talk artifacts seen in Fig. 1B (left), for example, represent current flow from the lower-resistance reference electrode through the interelectrode capacitance into the  $K^+$  barrel (Dick, E., and R. F. Miller, unpublished findings). The use of direct-capacitance neutralization improves the reference electrode response and reduces cross-talk artifacts in the  $K^+$  channel, as shown in Fig. 1B (center). A much greater reduction of cross-talk artifacts is achieved by switching to cross-capacitance neutralization, as shown in Fig. 1B (right). The application of cross-capacitance neutralization for electrophysiological purposes dates, at least, to the work of Frank et al. (1959), Frank and Becker (1964), and Tomita and Kaneko (1965), but it is interesting to note the recent suggestion of Dr. Alan Finkel (personal communication) that cross-capacitance neutralization, as used in the present study, acts to enhance interelectrode capacitance. Enhancing

interelectrode capacitance will make the time constants of both barrels more alike and thereby reduce artifacts by increasing the effectiveness of the amplifier common mode rejection function. Because of its superior efficacy in reducing cross-talk artifacts, the cross-capacitance neutralization capability of this amplifier was used in order to record

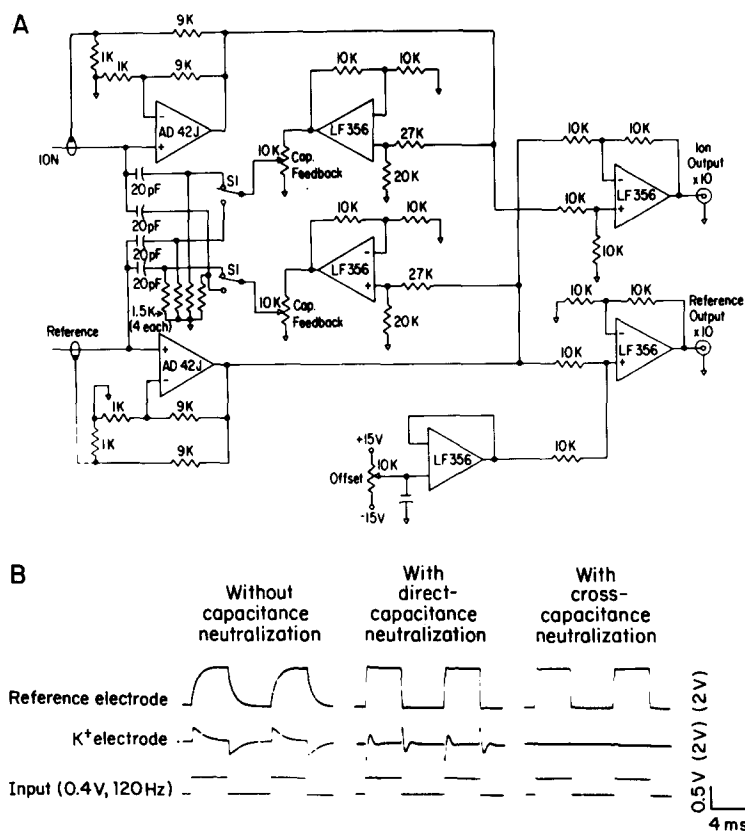


FIGURE 1. (A) Circuit diagram of the preamplifier used for recording from double-barreled  $K^+$ -selective microelectrodes. This amplifier possesses capabilities for direct- or cross-capacitance neutralization. (B) Photographic reproductions of storage oscilloscope displays, which show the output response of a double-barreled  $K^+$ -selective microelectrode, recorded through the preamplifier illustrated in A, to a 400-mV, 120-Hz square-wave test signal: (a) without capacitance neutralization (left); (b) using maximally adjusted direct-capacitance neutralization (center); and (c) using maximally adjusted cross-capacitance neutralization (right). Minimum "cross-talk" in the  $K^+$  electrode channel is achieved with cross-capacitance neutralization.  $K^+$  electrode: differential voltage recorded between the reference and  $K^+$ -selective barrels.

light-evoked  $K^+$  modulations minimally contaminated by the ERG potentials. The output from this preamplifier was led to the same group of secondary amplifiers and recorders as the first preamplifier. For the experiment illustrated in Figs. 4 and 5, the output of the preamplifier was also led through a signal averager (4800, DAGAN Corp., Minneapolis, MN) to a second display oscilloscope.

### *Preparation of Histological Sections*

Freshly excised eyecup preparations were: (a) fixed in 2.5% glutaraldehyde in amphibian Earle's solution for 2 h at room temperature; (b) washed three times for 5 min each in 0.1 M cacodylate buffer, pH 7.4; (c) fixed in 1% osmic acid in 0.1 M cacodylate buffer for 1 h at room temperature; (d) dehydrated through an alcohol series (10, 30, 50, 70, 95, 100, and 100% ethanol, 100% tertiary butyl alcohol); (e) embedded in araldite (grade CY-212, Polysciences, Inc., Warrington, PA); and (f) cut at 1- $\mu$ m sections.

## RESULTS

### *Depth Profile Studies*

Fig. 2A presents intraretinal ERGs and  $K_0^+$  modulations recorded simultaneously, using capacitance neutralization, during the withdrawal of a double-barreled  $K^+$ -selective microelectrode in a superfused *Bufo marinus* eyecup. Responses were evoked using 13-s stimuli of 533-nm light presented at 60-s intervals. Voltage signals in proximal retina are small because of the vitreal surface-to-ground shunt in this preparation. The traces of Fig. 2A are displayed as a function of relative retinal depth using the vitreal surface as a value of 0% and the R membrane (Brindley and Hamasaki, 1963; Cohen, 1965) as a value of 100%. In these studies, the position of the R membrane was determined by advancing the microelectrode through the distal retina until: (a) the reference electrode registered an abrupt, large voltage drop; (b) the amplitude of the intraretinal b-wave became markedly reduced; and (c) no light-evoked  $K_0^+$  response was detected. The microelectrode was then withdrawn until the DC voltage drop and ERG changes reversed and the  $K^+$  electrode response showed light-evoked  $K_0^+$  modulations characteristic of the subretinal space. The transition between the two sets of conditions, outlined above, occurred sharply over a distance of 5–10  $\mu$ m. The distal margin of this transition zone was taken to represent the R membrane.

In the distal retina, the ERG consists of a negative b-wave at light onset and a smaller negative d-wave at light offset, as indicated in the figure. The most distal light-evoked  $K_0^+$  change consists of a gradual decrease and return to baseline at light offset. The  $K_0^+$  decrease response goes through a maximum and progressive decline between the R membrane and middle retina. At 81% retinal depth, a transient, light-evoked  $K_0^+$  increase is seen (arrow 1) and successively larger  $K_0^+$  increases are seen at more proximal retinal levels. In this experiment, the light-evoked  $K_0^+$  increase reached a maximum at 41% retinal depth and then declined progressively from its maximum to the vitreal surface. In evaluating light-modulated  $K_0^+$  changes, it is important to know that  $K_0^+$  levels in the dark are not uniform throughout the retina (see the section on transretinal  $K_0^+$  gradient). Because of this, the relative sizes of light-evoked  $K_0^+$  changes measured at different retinal depths are not strictly represented by the  $K^+$  electrode responses. The magnitudes of the  $K_0^+$  changes can be calculated from the calibration curve of the electrode when more accurate comparisons are desirable. As an example, on the basis of  $K^+$  electrode responses, the light-evoked  $K_0^+$  increase at 61% retinal depth appears to be 31% as large as the maximum  $K_0^+$  increase. However, when calculated  $K_0^+$  changes are compared, the  $K_0^+$  increase at 61% retinal depth (0.14

meq/liter) is seen to be 56% as large as the maximum  $K_0^+$  increase at 41% retinal depth (0.25 meq/liter).

Fig. 2B presents a cross-section of *Bufo marinus* retina and is shown in order to help associate depth profile records of intraretinal ERGs and  $K_0^+$  modulations

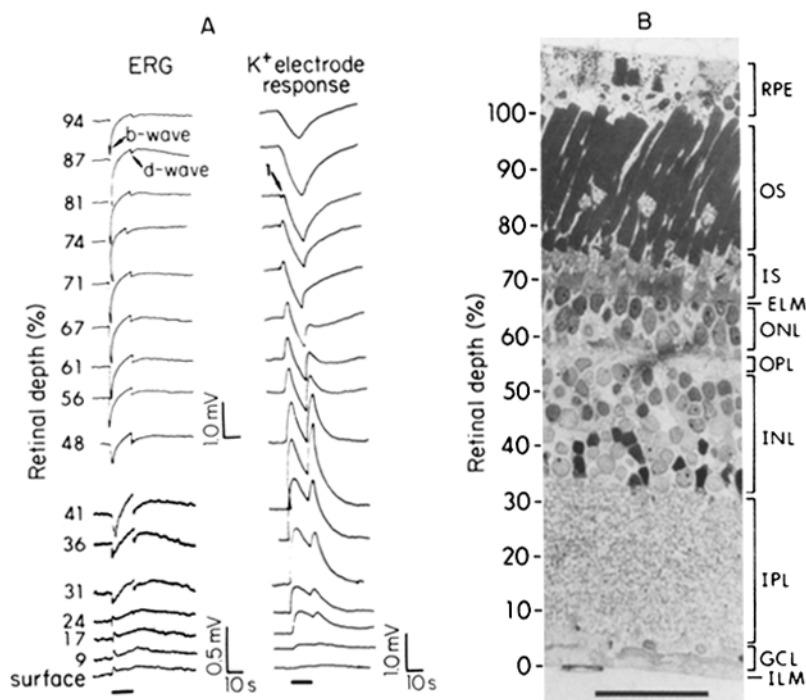


FIGURE 2. (A) Simultaneous recordings of the intraretinal ERG and  $K^+$  electrode responses taken at various retinal depths, expressed as percent retinal depth, during a microelectrode withdrawal in a superfused eyecup of the toad, *Bufo marinus*. Recordings were made using maximally adjusted cross-capacitance neutralization. A light-evoked  $K_0^+$  increase (arrow 1) is clearly seen at 81% retinal depth. Proximal ERG records are small in amplitude because of a vitreal surface-to-ground shunt in this preparation. The horizontal bar at the bottom of each column indicates the duration of the diffuse, 533-nm light stimulus. Irradiance:  $3.2 \times 10^{-7}$  W/cm<sup>2</sup>. (B) Cross-section from a retina of *Bufo marinus*. Abbreviations: RPE: retinal pigment epithelium; OS: outer segments; IS: inner segments; ELM: external limiting membrane; ONL: outer nuclear layer; OPL: outer plexiform layer; INL: inner nuclear layer; IPL: inner plexiform layer; GCL: ganglion cell layer; ILM: internal limiting membrane. Calibration bar, 50  $\mu$ m.

with the anatomical layers of the retina. The intraretinal ERGs and  $K^+$  electrode responses in Fig. 2A can be related to retinal levels as shown in Fig. 2B on the basis of percent retinal depth. A comparison between Figs. 2A and 2B shows that maximum light-evoked  $K_0^+$  increases occur near the level of the inner margin of the inner nuclear layer (INL) and in the inner plexiform layer (IPL). This finding is consistent with a previous report in which intraretinal dye injections

were used to localize  $K_o^+$  increases occurring in frog retina (Karwoski et al., 1978). Fig. 2 also shows that light-evoked  $K_o^+$  increases can be detected between the vitreal surface and retinal levels distal to the outer plexiform layer (OPL). We reported previously (Dick and Miller, 1978a) that there is a similar distribution of light-evoked  $K_o^+$  increases in mudpuppy retina. During the present study, additional depth profiles collected from retinas of toad, mudpuppy, and tiger salamander, as well as from frog (*Rana pipiens*) and bullfrog (*Rana catesbeiana*), were found to be qualitatively similar regarding the localization of peak  $K_o^+$  increases and the radial domain over which  $K_o^+$  increases were detected.

#### *Light-evoked $K_o^+$ Decrease and Slow PIII*

The light-evoked  $K_o^+$  decrease is primarily associated with a reduction of  $K^+$  efflux from photoreceptors (Oakley, 1975; Oakley and Green, 1976; Oakley et al., 1979; Steinberg et al., 1980) and has been proposed to initiate slow PIII through a passive,  $K^+$ -mediated hyperpolarization of Müller cell processes (Faber, 1969; Zuckerman, 1973; Witkovsky et al., 1975; Oakley, 1977; Karwoski and Proenza, 1977; Lurie and Marmor, 1980). One well-characterized pharmacological technique that can be used to test the Müller cell hypothesis of slow PIII generation is the application of cobalt ( $Co^{++}$ ) to block chemically mediated synaptic transmission (Weakly, 1973; Cervetto and Piccolino, 1974; Dacheux and Miller, 1976; Dacheux et al., 1979). In the presence of  $Co^{++}$ ,  $K_o^+$  modulations in the distal retina can be studied in isolation from post-receptor neuronal activity (Dick, 1979). According to the above hypothesis, one would predict that the  $Co^{++}$ -isolated, photoreceptor-generated  $K_o^+$  decrease would hyperpolarize Müller cells in a fashion that is proportional to the magnitude of the  $K_o^+$  response. An experiment carried out to test this prediction is shown in Fig. 3, which illustrates the effects of  $Co^{++}$  on the  $K_o^+$  decrease and Müller cell responses, as well as on the intraretinal ERG, in a tiger salamander eyecup.

In this experiment, a double-barreled  $K^+$ -selective micropipette was positioned in the distal retinal to record the intraretinal ERG and light-evoked  $K_o^+$  changes. Simultaneously, a second, single-barreled micropipette was used to record the light responses of a Müller cell, identified by its large resting membrane potential and characteristic on and off light responses. Control responses are shown on the left-hand side of Fig. 3A. Control records were obtained before superfusion was initiated because, for reasons that are not quantitatively understood, Müller cell responses recorded near the internal limiting membrane in superfused preparations are very attenuated in comparison with Müller cell responses recorded under nonsuperfusion conditions (Karwoski and Proenza, 1980; Miller, R. F., unpublished observations). The upper left-hand trace in Fig. 3A shows the light response from a Müller cell with a resting membrane potential of  $-92$  mV. The middle trace shows the intraretinal ERG and the lower trace shows the  $K^+$  electrode response. As seen in the middle trace, the intraretinal ERG at light onset consists of a positive a-wave followed by a negative b-wave. The slow positivity (labeled "slow PIII") seen after the b-wave is presumed to be slow PIII, based on the consistent observation throughout all of our studies that the null, or inversion, point for this response always occurred much more proximally than the inversion point for the a-wave. However, given our recording configuration,

we cannot exclude a mass receptor potential contribution to this slow positivity. A response amplitude (expressed as  $V/V_{\max}$ ) vs.  $\log I$  series was generated for the  $K_0^+$  decrease and slow PIII responses, measured from baseline to peak, at eight intensity levels. The data are illustrated graphically on the left of Fig. 3B.

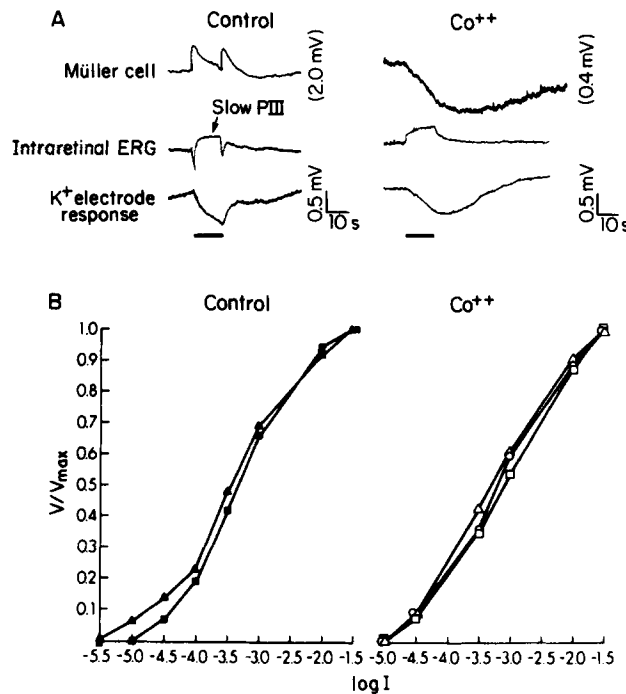


FIGURE 3. (A) Effects of  $\text{Co}^{++}$  on the intraretinal ERG, light-evoked  $\text{K}_0^+$  decrease, and intracellularly recorded Müller cell responses; simultaneous recordings were from freshly excised tiger salamander eyecup. A double-barreled micropipette was positioned in the outer retina to record the intraretinal ERG and light-evoked  $\text{K}_0^+$  modulations with cross-capacitance neutralization. Simultaneously, a second, single-barreled micropipette was used to record the light response of a Müller cell. Control responses are shown to the left. The traces in the right-hand column show the effects of superfusion with 5 mM  $\text{CoCl}_2$ : the Müller cell light response consists of a slow hyperpolarization; the ERG consists of a-wave and slow PIII. Diffuse white light stimuli. Irradiance:  $3.2 \times 10^{-7} \text{ W/cm}^2$ . (B) Plots of the normalized amplitude vs.  $\log I$  relationships for the responses shown in A. The left side shows the amplitude vs.  $\log I$  relationships for slow PIII and light-evoked  $\text{K}_0^+$  decrease under control conditions. The right side shows the amplitude vs.  $\log I$  relationships for the Müller cell response (O), slow PIII ( $\blacktriangle$ ), and the light-evoked  $\text{K}_0^+$  decrease ( $\blacksquare$ ,  $\square$ ) measured during  $\text{Co}^{++}$  application. Maximum irradiance (0.0):  $3.2 \times 10^{-4} \text{ W/cm}^2$ .

Threshold for detection of the  $\text{K}^+$  electrode response was 0.5 log units higher than that for detection of the ERG response. Beyond this difference, the two responses exhibited parallel amplitude vs.  $\log I$  properties over the remaining 3.5 log unit range of intensities tested.

After the control records were obtained, superfusion of the preparation with

a Ringer's solution containing 5 mM  $\text{CoCl}_2$  was initiated. Within 1 min, the extracellularly recorded responses consisted of only the  $\text{K}_o^+$  decrease and an intraretinal ERG having an initial rapid positivity (a-wave) followed by a slower positivity (slow PIII) with a reversal of this sequence at light offset. A second Müller cell was impaled and identified by its large resting membrane potential and the fact that Müller cell recordings are most commonly obtained near the vitreal surface of the retina, the recording locus for the Müller cell responses in Fig. 3. Amplitude vs.  $\log I$  data were then collected at six different light intensities for the ERG,  $\text{K}^+$  electrode, and Müller cell responses. The right-hand column of Fig. 3A illustrates responses obtained with the same light intensities used for the control responses. The light stimulus evoked a hyperpolarization in the Müller cell with a time course similar to that of the  $\text{K}_o^+$  decrease. Later, when the intracellular pipette was moved to an adjacent extracellular position, no light-evoked activity was observed, which indicates that the intracellularly recorded response represented Müller cell transmembrane current flow (data not shown). Amplitude vs.  $\log I$  data for the slow PIII,  $\text{K}_o^+$  decrease, and Müller cell responses during  $\text{Co}^{++}$  treatment are shown on the right-hand side of Fig. 3B. The three responses were seen to behave in a parallel fashion over the 3.5 log units of light intensities tested. Four additional  $\text{Co}^{++}$  application experiments like that illustrated in Fig. 3 also showed  $V/V_{\max}$  vs.  $\log I$  curves for the Müller cell hyperpolarization, slow PIII, and  $\text{K}_o^+$  decrease responses, which closely paralleled one another within each experiment. These results are consistent with the hypothesis that a light-evoked  $\text{K}_o^+$  decrease hyperpolarizes Müller cell processes in the distal retina and gives rise to a current flow detected as the slow PIII component of the ERG.

#### *Light-evoked $\text{K}_o^+$ Increases*

**LATENCY MEASUREMENTS** The present and previous studies have shown that light-evoked  $\text{K}_o^+$  increases can be detected at retinal levels corresponding to all but the most distal 20–30% of retinal depth (Dick and Miller, 1978a; Kline et al., 1978; Dick, 1979; Karwoski et al., 1982; Shimazaki et al., 1984). Are the  $\text{K}_o^+$  increases detected in the distal retina simply manifestations of  $\text{K}^+$ , which has diffused from more proximal release sites, or do the  $\text{K}_o^+$  increases in distal vs. proximal retina reflect the activity of predominantly different populations of retinal neurons? Measurements of latencies vs. retinal depth provide one approach to discriminating between these alternatives.

Fig. 4 shows selected points from a latency vs. depth analysis for intraretinal ERGs and  $\text{K}^+$  electrode responses in a *Bufo marinus* eyecup. These data were collected using capacitance neutralization and largely the same procedure as the depth profile data of Fig. 2A, but with the following differences: (a) responses were evoked by white light stimuli; (b) the duty cycle for the light stimulus was 5 s on and 35 s off; and (c) ERGs and  $\text{K}^+$  electrode responses were led to a signal averager as well as to a penwriter. Fig. 4A shows paired penwriter records of the intraretinal ERG (labeled "ERG") and  $\text{K}^+$  electrode response (labeled " $\text{K}^+$ ") from seven selected retinal depths. The light stimulus duration is indicated by the solid bar at the bottom of the column. At each retinal level, a series of four pairs of light-evoked responses was signal-averaged and subsequently displayed on an

oscilloscope at a higher gain and faster sweep speed than the penwriter records. Fig. 4B presents photographically reproduced oscilloscope records of the signal-averaged responses. Each ERG and K<sup>+</sup> electrode trace in B corresponds to a

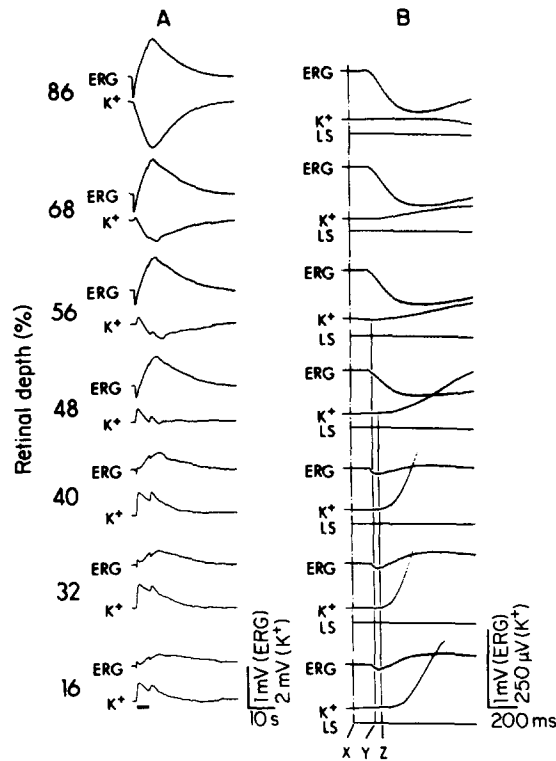


FIGURE 4. Latency vs. depth analysis for intraretinal ERGs (labeled "ERG") and K<sup>+</sup> electrode responses (labeled "K<sup>+</sup>") in a *Bufo marinus* eyecup. Recordings were made using capacitance neutralization. Column A shows paired penwriter records of the intraretinal ERGs and K<sup>+</sup> electrode response at seven retinal depths. The bar beneath column A denotes the duration of the diffuse white light stimulus. Column B shows oscilloscope records of the first 850 ms of four signal-averaged responses corresponding to the penwriter record to its left in A. The light stimulus onset was also recorded through the signal averager and displayed on the oscilloscope as the appearance of the trace labeled "LS." The line marked "X" aligns arbitrary but time-invariant markers inserted into the oscilloscope traces by the signal averager. The markers, seen as a dot over each trace, were set to coincide with the onset of the light stimulus. The line marked "Y" denotes the latency of the light-evoked K<sub>0</sub><sup>+</sup> increase at 56% retinal depth. The line marked "Z" denotes the latencies of the light-evoked K<sub>0</sub><sup>+</sup> increases at 40 and 32% retinal depths, which were too close to differentiate. The light-evoked K<sub>0</sub><sup>+</sup> increase at 56% retinal depth has a latency shorter by ~40 ms, in this case, than the peak proximal K<sub>0</sub><sup>+</sup> increases. Diffuse white light stimuli. Irradiance:  $3.2 \times 10^{-7}$  W/cm<sup>2</sup>.

penwriter record to its left in A and shows the first 850 ms of the related response. All responses were evoked by identical light stimuli. The light stimulus onset was also recorded through the signal averager and displayed on the

oscilloscope (the line labeled "LS"). The line marked "X" aligns arbitrary but time-invariant markers inserted into the traces by the signal averager. The markers, seen as a dot over each trace in *B*, were set to coincide with the onset of the light stimulus. The line marked "Y" denotes the latency (estimated by eye) of the light-evoked  $K_o^+$  increase measured at 56% retinal depth. The line marked "Z" denotes the latencies of the light-evoked  $K_o^+$  increases at 40 and 32% retinal depths, which were too close to be readily differentiated. Several features of Fig. 4*B* should be emphasized. First, the shortest-latency  $K_o^+$  increase (~130 ms) was seen at 56% retinal depth, despite the fact that the response was smaller and had a slower rate of rise than more proximal  $K_o^+$  increases. Second, the  $K_o^+$  increase at 56% retinal depth is "bracketed" by longer-latency  $K_o^+$  increases both distal (~170 ms at 68% retinal depth) and proximal to it (~200 ms at 48% retinal depth). Third, the  $K_o^+$  increases at 40 and 32% retinal depths (latencies of ~170 ms) were jointly bracketed, distally and proximally, by longer-latency  $K_o^+$  increases. These three features of the latency data indicate two reasons why there must be more than one source of light-evoked  $K^+$  release in the retina. First, the shortest-latency  $K_o^+$  increase at 56% retinal depth cannot simply represent  $K^+$  that has diffused into the outer retina from a more proximal release site, because, in that case, it would have a longer latency than proximal  $K_o^+$  increases. Second, because the  $K_o^+$  increases at both distal (56%) and proximal (40 and 32%) retinal depths are bracketed by longer-latency  $K_o^+$  increases, these responses can be seen to describe relative latency minima with respect to retinal depth, as previously described by Karwoski and Proenza (1982) and Karwoski et al. (1982). Having two latency minima requires having two independent sources of light-evoked  $K^+$  release at different retinal levels. On the basis of percent retinal depth and in agreement with Karwoski et al. (1982), one of these sources appears to occur near the level of the OPL, while the second is distributed in the IPL and around the IPL-INL margin.

Five of six completed analyses of latency vs. depth in *Bufo marinus* retina showed both a distal  $K_o^+$  increase, which was smaller but of shorter latency than peak proximal  $K_o^+$  increases, and a region of longer-latency  $K_o^+$  increases, which occurred between the peak proximal  $K_o^+$  responses and the distal, shorter-latency  $K_o^+$  increase. In one analysis, the  $K_o^+$  increase occurring near the OPL showed a latency longer by ~40 ms than the peak proximal  $K_o^+$  response. However, distal and proximal regions of light-evoked  $K^+$  release were still separable on the basis of light-evoked  $K_o^+$  increases at intermediate retinal depths that showed longer latencies than the distal  $K_o^+$  response in that instance.

For latency analyses, it is crucial to know whether or not the  $K^+$  electrode responses are contaminated with artifactual b-waves. Therefore, we examined the effectiveness of our capacitance neutralization techniques to eliminate artifactual b-waves in the  $K^+$  electrode channel by comparing ERGs and  $K^+$  electrode responses recorded with and without capacitance neutralization. This was readily accomplished during experiments such as the one illustrated in Fig. 4 by recording light-evoked responses at each retinal depth and then switching out the capacitance neutralization circuits of the amplifier and immediately re-recording the intraretinal ERG and  $K^+$  electrode response at that same level. Fig. 5 shows

such a comparison taken from the experiment illustrated in Fig. 4. In Fig. 5, the upper sets of responses in *A* and *B* are the same data shown in Fig. 4 at 68% retinal depth and were recorded with capacitance neutralization as indicated. The lower sets of penwriter traces and signal-averager records were generated under identical conditions, within 200 s of those shown above them, with the exception that capacitance neutralization was not used. As in Fig. 4, the line marked "X" aligns time-invariant markers inserted into the oscilloscope traces by the signal averager, which were set to coincide with the onset of the light

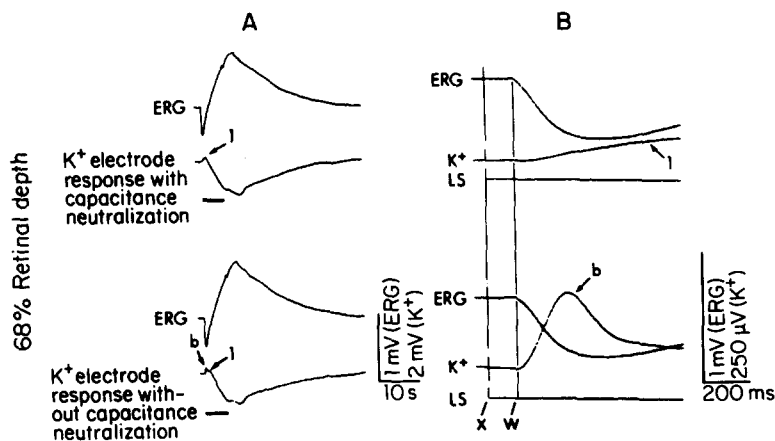


FIGURE 5. Comparison of intraretinal ERGs (labeled "ERG") and  $K^+$  electrode responses (labeled " $K^+$ ") recorded with and without the use of cross-capacitance neutralization. Upper sets of penwriter traces (column *A*) and oscilloscope records (column *B*) are the same data shown in Fig. 4 at 68% retinal depth. The lower sets of records in columns *A* and *B* were measured within 200 s of the corresponding trace above them and are identical, except that they were recorded without capacitance neutralization. As in Fig. 4, the line marked "X" aligns time-invariant markers inserted into the oscilloscope traces by the signal averager, which were set to coincide with the onset of the light stimulus (appearance of the line labeled "LS"). The line labeled "W" denotes the b-wave latencies, which were identical in both upper and lower oscilloscope records. As described in the text, the response labeled "1" is a light-evoked  $K_0^+$  increase, while response labeled "b" is an artifactual b-wave appearing in the  $K^+$  electrode response. Note that in column *B*, "b" and the b-wave have an identical latency. Diffuse white light stimuli. Irradiance:  $3.2 \times 10^{-7}$  W/cm<sup>2</sup>.

stimulus. The line labeled "W" denotes b-wave latencies, which are identical in both upper and lower oscilloscope records. The first light-evoked change seen in the  $K^+$  electrode responses recorded with capacitance neutralization is a positivity labeled "1." The oscilloscope record in *B* shows that response 1 has both a longer latency and time to peak than the b-wave. In contrast, the first light-evoked change seen in the  $K^+$  electrode response recorded without capacitance neutralization is a relatively fast-rising positivity (labeled "b"), which overlaps into the slower positivity (1) described above. The oscilloscope record reveals that *b* has an identical latency and shorter time to peak than the b-wave. On the

basis of its appearance when capacitance neutralization is removed and its parallel latency to the ERG response, we conclude that positivity *b* is an artifactual b-wave in the  $K^+$  electrode record. Positivity 1 appears, then, to be a light-evoked  $K_0^+$  increase. By looking at the  $K^+$  electrode response at 86% retinal depth in Fig. 4, one can see why response 1 is a  $K_0^+$  increase and not simply an attenuated artifactual b-wave. At 86% retinal depth, light-evoked  $K_0^+$  increases are not detected and the  $K^+$  electrode response recorded with capacitance neutralization is seen to be flat during the period of the b-wave. From these results, we conclude that artifactual b-waves resulting from the different time constants of the two electrodes are effectively eliminated from the  $K^+$  electrode responses recorded with cross-capacitance neutralization and that our latency measurements of light-evoked  $K_0^+$  increases were not influenced by artifactual b-waves. It is also evident from the lowest left-hand trace of Fig. 5 that artifactual b-waves can be readily distinguished from light-evoked  $K_0^+$  increases in penwriter records collected without capacitance neutralization techniques.

**PHARMACOLOGICAL SEPARATION OF LIGHT-EVOKED  $K^+$  INCREASES** Latency measurements suggest that different neuronal populations contribute to light-evoked  $K_0^+$  increases in distal vs. proximal retina. Pharmacological techniques can also be used to discriminate between different sources of light-evoked  $K^+$  release. We previously reported that glycine, ethanol, and the combination of  $\gamma$ -aminobutyric acid (GABA) plus ethanol can differentially modulate the activity of subpopulations of retinal neurons that appear to underlie the relatively distal vs. proximal  $K_0^+$  responses in mudpuppy retina (Dick and Miller, 1978*a*; Dick, 1979). Shimazaki et al. (1983, 1984) have reported similar actions of both GABA plus ethanol and aspartate. In Figs. 6 and 7, we show that GABA and  $\alpha$ -aminopimelic acid (APA) can also be used to separate the light-evoked  $K_0^+$  increase into distal and proximal components.

**GABA** A putative retinal transmitter role for GABA has been suggested by histochemical and autoradiographic techniques (Lam and Steinman, 1971; Starr and Voaden, 1972; Lam, 1976), biochemical studies (Berger et al., 1977; Kennedy et al., 1977), and electrophysiological investigations (Straschill and Perwein, 1969; Miller et al., 1977, 1981*a, b*; Caldwell et al., 1978). In mudpuppy, GABA shows selectivity for the on vs. the off channel of neuronal information processing (Miller et al., 1977, 1981*a, b*).

Fig. 6 illustrates the effects of 2 mM GABA on intraretinal ERGs and  $K^+$  electrode responses measured in a superfused mudpuppy eyecup during a single microelectrode withdrawal. The protocol for this experiment and that of Fig. 7, which illustrates APA effects, was as follows. A double-barreled  $K^+$ -selective micropipette was positioned in the outer retina at the most distal level where a distinct light-evoked  $K_0^+$  increase was evident in the  $K^+$  electrode response. This outermost retinal level was used to minimize contributions to the light-evoked  $K_0^+$  increase from proximal sources of  $K^+$  release. Once the microelectrode was positioned, control responses for the ERG and distal light-evoked  $K_0^+$  increase were recorded. The perfusate was then switched to a Ringer's solution that contained the test agent and light responses were again recorded. 3–4 min after introducing the test agent, the control Ringer's was reintroduced and the light

responses were recorded. The micropipette was then withdrawn to a retinal level near the maximal proximal  $K_0^+$  increase and the experiment was repeated. For statistical purposes, each set of distal and proximal responses was considered to be one trial. Repeated applications of an agent during a single microelectrode penetration were not considered to be individual trials but always gave highly reproducible results. In this set of experiments (Figs. 6 and 7), cross-capacitance neutralization was not used and, therefore, artifactual b-waves occur in the  $K^+$  electrode responses (arrow labeled "b").

In the experiment illustrated in Fig. 6, exposure to GABA caused a slight reduction in the b-wave and the distal light-evoked  $K_0^+$  increase (arrow 1).

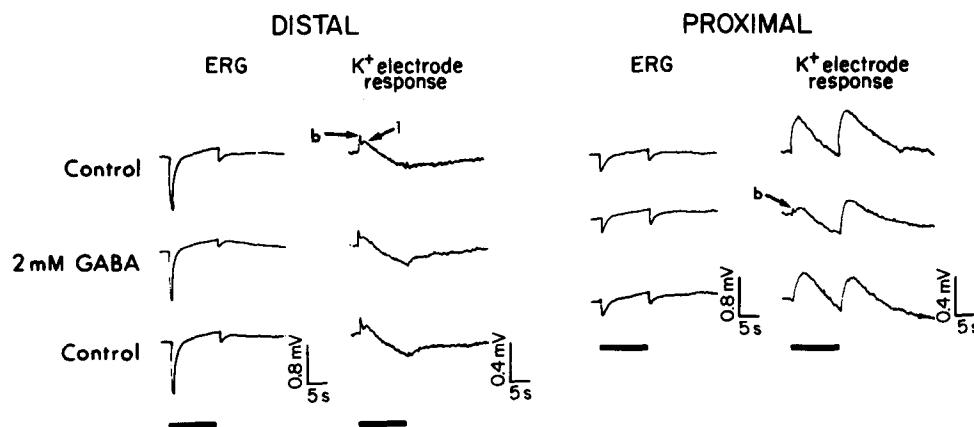


FIGURE 6. Effects of 2 mM GABA on intraretinal ERGs and  $K^+$  electrode responses recorded (without capacitance neutralization) in the distal (left) and proximal (right) retina of a mudpuppy eyecup. Exposure to GABA (center traces) caused a slight reduction in both the distal light-evoked  $K_0^+$  increase (arrow 1) and b-wave, while it dramatically reduced the proximal  $K_0^+$  increase at light onset and caused a smaller reduction of the proximal  $K_0^+$  increase at light offset. Arrows marked "b" indicate artifactual b-waves. Diffuse white light stimuli are indicated by horizontal bars. Irradiance:  $3.2 \times 10^{-7}$  W/cm<sup>2</sup>.

However, it reduced the proximal  $K_0^+$  increase at light onset by >80%. Light stimuli in these experiments were given at 60-s intervals and GABA effects were typically detected within a single stimulus cycle. The application of 2 mM GABA always reduced the magnitude of proximal  $K_0^+$  increases. However, in 8 of 20 experiments with mudpuppy preparations, the distal light-evoked  $K_0^+$  increase and b-wave were unaffected by exposure to GABA, and in 4 of 20 experiments, the b-wave and distal  $K_0^+$  increase were slightly enhanced. In 20 trials involving 10 mudpuppy eyecups, the b-wave and distal  $K_0^+$  increase were essentially unaffected by GABA. In GABA, the amplitudes of the b-wave and distal  $K_0^+$  increase were, respectively,  $98 \pm 10$  and  $97 \pm 7\%$  of control values. In the same set of 20 trials, the mean GABA-induced reduction of the proximal  $K_0^+$  increase at light onset was to  $19 \pm 7\%$  of control values. In addition, throughout these experi-

ments, as illustrated in Fig. 6, GABA more effectively depressed on vs. off  $K_0^+$  increases in the proximal retina. This last result is consistent with the greater GABA sensitivity of second- and third-order neuronal responses associated with the on vs. off channel of retinal information processing as demonstrated by Miller and co-workers (1977, 1981*a, b*).

**APA** APA [ $\text{HO}_2\text{C}(\text{CH}_2)_4\text{CH}(\text{NH}_2)\text{CO}_2\text{H}$ ] is a glutamate [ $\text{HO}_2\text{C}(\text{CH}_2)_2\text{CH}(\text{NH}_2)\text{CO}_2\text{H}$ ] analogue. An intracellular recording screen of APA actions on the retinal network of the mudpuppy (Dick, 1979) indicated that APA effects are dose-dependent and that at concentrations of  $\leq 1.0$  mM its influence appears to be restricted to a reduction of light responsiveness in amacrine and ganglion cells.

Fig. 7 illustrates the effects of exposure to 0.8 mM APA upon intraretinal

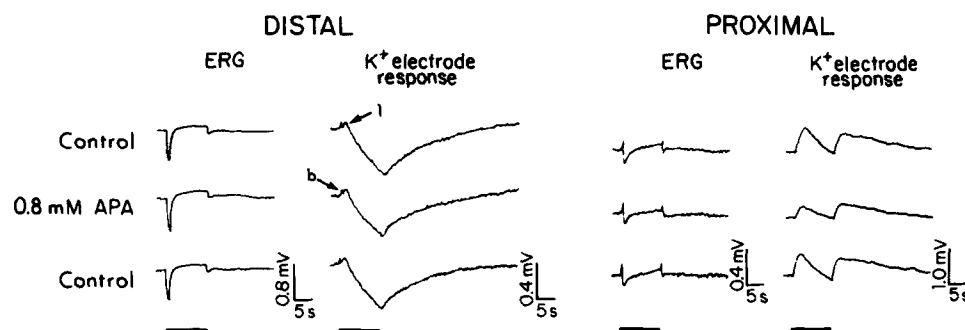


FIGURE 7. Effects of 0.8 mM APA on the intraretinal ERG and  $K_0^+$  electrode responses recorded (without capacitance neutralization) in the distal (left) vs. proximal (right) retina of a mudpuppy eyecup. The application (3–4 min) of 0.8 mM APA had no effects on the distal light-evoked  $K_0^+$  increase (arrow 1) or the b-wave. The negative off response of the ERG, recorded in proximal retina, is slightly prolonged during APA exposure. In contrast, the proximal  $K_0^+$  increases at light onset and offset are reduced by about one-half. Arrow "b" indicates the artifactual b-wave. Diffuse white light stimuli are indicated by horizontal bars. Irradiance:  $3.2 \times 10^{-7}$  W/cm<sup>2</sup>.

ERGs and distal and proximal  $K_0^+$  responses measured in a superfused mudpuppy eyecup during a single microelectrode withdrawal. APA is seen to have no effect upon the ERG and distal light-evoked  $K_0^+$  increase. However, the proximal  $K_0^+$  increases at both light onset and offset are reduced by about one-half (note gain change). As was the case with exposure to GABA, proximal  $K_0^+$  increases were always reduced by APA (17 of 17 trials), while the distal  $K_0^+$  increase and b-wave were either unaffected (8 of 17 trials) or showed a slight reduction or enhancement. In 17 trials involving 11 mudpuppy eyecups, the mean effect induced by the application of 0.8–1.0 mM APA was a reduction in the b-wave and distal  $K_0^+$  increase to, respectively,  $99 \pm 7$  and  $100 \pm 11\%$  of the control values. In the same set of 17 trials, the mean APA-induced reduction of the proximal  $K_0^+$  increase at light onset was to  $51 \pm 12\%$  of the control values. These observations further support the view, indicated by experiments with ethanol, ethanol plus

GABA, glycine, aspartate (Dick and Miller, 1978a; Dick, 1979; Shimazaki et al., 1983), and GABA, that activities of predominantly different populations of retinal neurons underlie light-evoked  $K_o^+$  increases at distal as opposed to proximal retinal levels.

#### The Transretinal $K_o^+$ Gradient

The extracellular environment of the vertebrate retina is not uniform with respect to  $K_o^+$ . Maximum  $K_o^+$  occurs in the outer retina and progressively declines toward the vitreal surface (Oakley, 1975; Dick, 1979; Steinberg et al., 1980).

Using  $K^+$ -selective microelectrode techniques, Oakley (1975) and Oakley and Green (1976) demonstrated transretinal  $K_o^+$  gradients of 2.2–2.8 mM in the frog

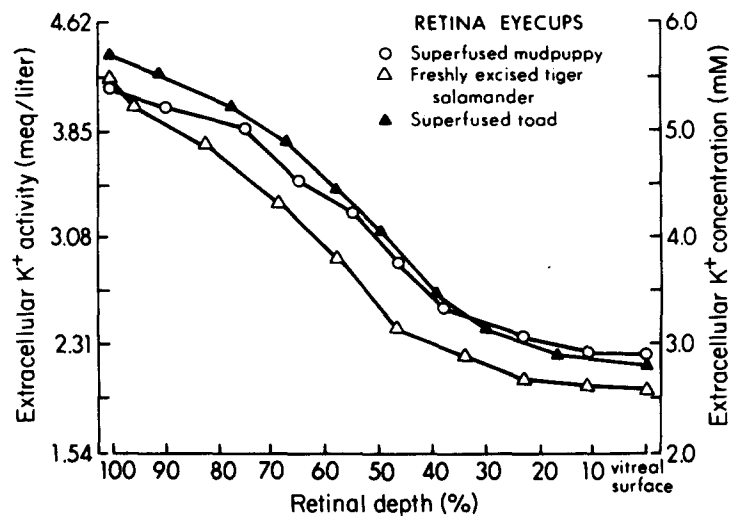


FIGURE 8. Representative transretinal  $K_o^+$  gradients from mudpuppy (*Necturus maculosus*), tiger salamander (*Ambystoma tigrinum*), and toad (*Bufo marinus*). Extracellular  $K^+$  values are expressed in units of both activity (milliequivalents per liter) and concentration (millimolar).

retina, with concentrations at the vitreal surface of  $\sim 2.8$  mM. In the present study, transretinal  $K_o^+$  gradients were measured in dark-adapted mudpuppy, tiger salamander, and toad retinas. Fig. 8 illustrates representative transretinal extracellular  $K^+$  gradients from these species. Extracellular  $K^+$  values are expressed here in units of both activity (milliequivalents per liter) and concentration (millimolar) for purposes of convenient comparisons with the data from other laboratories. Fig. 8 illustrates that these amphibian (I-type) retinas all exhibit transretinal  $K_o^+$  gradients of similar form and magnitude, and with vitreal  $K_o^+$  values in the range of 1.9–2.2 meq/liter ( $\sim 2.5$ – $2.9$  mM). The magnitude of their transretinal  $K_o^+$  gradients closely approximates those previously reported in frog (Oakley, 1975). We have not examined transretinal  $K_o^+$  gradients in light-adapted retinas.

## DISCUSSION

*Light-evoked  $K_o^+$  Decrease*

Our results are in full agreement with previous studies (Oakley, 1975, 1977; Oakley and Green, 1976; Tomita, 1976; Karwoski and Proenza, 1977, 1978; Dick and Miller, 1978*a, b*; Kline et al., 1978; Matsuura et al., 1978; Steinberg et al., 1980; Vogel, 1980) in finding a light-evoked  $K_o^+$  decrease that is maximal in the distal retina. Oakley (1975, 1977) and other workers (Oakley and Green, 1976; Steinberg et al., 1980; Vogel, 1980) have demonstrated, in rod-dominated retinas, that the  $K_o^+$  decrease is a rod-dominated phenomenon and that it initiates the RPE component of the c-wave through a passive hyperpolarization of the apical membrane of pigment epithelial cells. In some species, cone contributions to the  $K_o^+$  decrease are suggested by cone-dominated c-waves (Tigges et al., 1967) and c-wave components (Matsuura et al., 1978).

**SLOW PIII** In an early ERG analysis, Noell (1953) described an "azide-insensitive potential," which had a time course similar to the c-wave but was of opposite polarity when recorded in the vitreous. This potential was later named "slow PIII" (Faber, 1969), a term that has been generally adopted to describe what can be viewed as a corneal-negative c-wave component originating within the neural retina (Faber, 1969; Oakley, 1977). Considerable evidence now supports the idea that the light-evoked  $K_o^+$  decrease gives rise to slow PIII by initiating a passive hyperpolarization of Müller cell processes in the distal retina, which in turn sets up a transretinal current flow detected as the slow pIII voltage (Faber, 1969; Zuckerman, 1973; Witkovsky et al., 1975). However, intracellular recordings from Müller cells in the mudpuppy do not generally show hyperpolarizing responses except very late during a prolonged light stimulus (Karwoski and Proenza, 1977, 1980; Dick, 1979). In the present study, we have shown that there is a light-evoked Müller cell hyperpolarization when  $Co^{++}$  is used to block chemically mediated synaptic transmission. The time course and amplitude-intensity relationship of the Müller cell hyperpolarization correspond closely to those of the extracellularly recorded  $K_o^+$  decrease. The findings strongly support the Müller cell hypothesis of slow PIII generation.

*Light-evoked  $K_o^+$  Increases*

The present study and previous reports (Dick and Miller, 1978*a*; Kline et al., 1978; Karwoski et al., 1982; Shimazaki et al., 1983, 1984) demonstrate that  $K^+$ -selective microelectrode techniques can detect light-evoked  $K_o^+$  increases in all but the most distal 20–30% of the retinas of mudpuppy, toad, tiger salamander, and skate. More recently, we have found a similar distribution of  $K_o^+$  increases in rabbit retina (Dick et al., 1985). A number of previous studies have characterized properties of the light-evoked  $K_o^+$  increase in proximal retina but have not distinguished a  $K_o^+$  increase in distal retina (Oakley, 1975; Oakley and Green, 1976; Tomita, 1976; Karwoski and Proenza, 1977, 1978; Vogel and Green, 1979, 1980; Vogel, 1980). Consequently, the primary question we addressed was whether or not the  $K_o^+$  increase detected in distal retina is simply a diffusional manifestation of  $K^+$  released from a more proximal retinal site. We have been able to discriminate between distal and proximal  $K_o^+$  increases on the bases of

response latencies and differential sensitivity to pharmacological agents. We conclude from such analyses that different neuronal mechanisms must underlie the generation of distal vs. proximal light-evoked  $K_0^+$  increases. Recently, Karwoski and Proenza (1982) and Karwoski et al. (1982) have made latency measurements of light-evoked  $K_0^+$  increases registered between the external and internal limiting membranes in frog and mudpuppy retinas. They report that analyses of  $K_0^+$  increase latency vs. depth reveal latency minima at the levels of the OPL and IPL. Our measurements in toad are consistent with their measurements in frog and mudpuppy; all support the conclusion that different neuronal sources contribute to light-evoked  $K_0^+$  increases at different retinal levels.

The most clear-cut evidence that light-evoked  $K_0^+$  increases can be regionalized into distal and proximal components comes from the use of pharmacological agents that exert selective actions upon the neuronal network. In the present study, we have shown that GABA and APA can be used to distinguish between distal and proximal sources of  $K^+$  release in the mudpuppy retina. Our results from experiments with GABA and APA are consistent with previous reports from this laboratory on the effects of glycine, ethanol, and the combination of ethanol plus GABA upon the b-wave and distal and proximal  $K_0^+$  increases (Dick and Miller, 1978a; Dick, 1979). During applications of these substances, b-waves and distal  $K_0^+$  increases were markedly enhanced, while proximal light-evoked  $K_0^+$  increases were either markedly depressed (ethanol, ethanol plus GABA) or relatively unaffected (glycine). Throughout our pharmacological studies, changes in the magnitude of the b-wave were always closely paralleled by changes in the magnitude of the distal  $K_0^+$  increase, but were never paralleled by changes in the proximal  $K_0^+$  increase. Shimazaki and co-workers (1983, 1984) also report a discrimination between distal and proximal light-evoked  $K_0^+$  increases in mudpuppy retina, based upon the pharmacological actions of either aspartate or the combination of GABA plus ethanol.

This study has shown that the distal light-evoked  $K_0^+$  increase is not an artifact of our recording conditions, as argued by Vogel (1980). Vogel characterized three electrical sources that can contribute artifacts to the  $K^+$  electrode response. Two of these are "stray" and "cross-capacitance"; the latter is derived from interelectrode capacitance. Vogel additionally discovered that if the microelectrode tip is sufficiently large and if it sits in a region of a large voltage gradient, the differential recording may measure the voltage difference between the two electrode tips. The ERG artifact that may appear in the  $K^+$  electrode signal as the result of this phenomenon, as well as those that are contributed by capacitance, will be closely time-locked with the ERG. The primary component of this overall artifact will be the b-wave, the largest of the higher-frequency ERG components. The characteristics of such an artifactual b-wave are shown on a fast time scale in Fig. 5. As shown in Figs. 4 and 5, artifactual b-waves were effectively eliminated from our  $K^+$  electrode responses recorded with the use of cross-capacitance neutralization. ERG artifacts do appear in our  $K^+$  electrode responses under recording conditions in which we do not use capacitance neutralization (Figs. 5-7). However, these artifacts are clearly distinguishable from the distal  $K_0^+$  increase recorded in penwriter records.

*Which Neuronal Populations Generate Distal and Proximal Light-evoked  $K_o^+$  Increases?*

**PROXIMAL LIGHT-EVOKED  $K_o^+$  INCREASE** A number of studies have already related the proximal  $K_o^+$  increase to amacrine and ganglion cell activity on the basis of the phenomenological and pharmacological properties of the  $K_o^+$  response (Oakley, 1976; Karwoski and Proenza, 1977, 1980; Karwoski et al., 1978; Dick and Miller, 1978*a, b*; Dick, 1979). The present study provides further support for this association, based upon the selective suppression of this  $K_o^+$  response by GABA (Fig. 6) and APA (Fig. 7). Intracellular recording studies in mudpuppy have shown that amacrine and ganglion cells are more GABA-sensitive than any other retinal neurons (Miller et al., 1977, 1981*a, b*) and that they are the only retinal neurons that are sensitive to APA at concentrations of  $\leq 1.0$  mM (Dick, 1979). Consequently, GABA- and APA-mediated suppressions of proximal  $K_o^+$  increases probably represent selective pharmacological actions upon amacrine and ganglion cells.

**DISTAL LIGHT-EVOKED  $K_o^+$  INCREASE** Retinal physiology suggests that the distal  $K_o^+$  increase must be related to depolarizing bipolar cell responses, since, in amphibians, depolarizing bipolars constitute the only class of retinal neurons that both have processes distributed in the OPL and depolarize to white light stimuli, such as those used through most of this study. An association between depolarizing bipolars and distal  $K_o^+$  increases would be consistent with the relative insensitivity to 1.0 mM APA of both the  $K_o^+$  response (Fig. 7) and the neuronal response (Dick, 1979).

The distal  $K_o^+$  increase and b-wave are also relatively insensitive to 2 mM GABA. In contrast to the relative insensitivity of depolarizing bipolars to APA, the light responses of these neurons are reduced by 2 mM GABA (Miller et al., 1981*a*). However, GABA actions upon depolarizing bipolars are associated with a conductance increase (Miller et al., 1981*a*). Thus, extracellular,  $K^+$ -mediated currents of depolarizing bipolar cell origin might be relatively unaffected by 2 mM GABA.

A depolarizing bipolar cell origin for the distal  $K_o^+$  increase has also been indicated by previous analyses of ethanol actions upon the retinal network (Dick, 1979), ERGs, and light-evoked  $K_o^+$  responses (Dick and Miller, 1978*a*), as well as by localizations of the distal  $K_o^+$  increase to the OPL (Karwoski et al., 1982).

*$K_o^+$  Increases and the B-Wave*

The Müller cell theory of Faber (1969) and Miller and Dowling (1970*a*) proposed that the b-wave is initiated by a light-evoked  $K_o^+$  increase that depolarizes Müller cell processes at the level of the OPL. Within the last decade, alternative hypotheses to the Müller cell theory have been proposed, primarily in association with  $K^+$ -selective microelectrode studies whose findings have not agreed with predictions of the glial theory (Oakley, 1975; Karwoski and Proenza, 1978; Vogel, 1980; Yanagida and Tomita, 1982). An idea common to the alternative theories is that depolarizing bipolar cell responses directly generate part or all of the b-wave. The results of the present study are not sufficient to distinguish whether any phase of the b-wave is generated directly by neuronal responses or

secondarily via K<sup>+</sup>-mediated influences on Müller cells. However, after the work of Faber (1969) and Miller and Dowling (1970*a, b*), additional support for the Müller cell theory of b-wave generation has come from current source density analyses (Proenza and Freeman, 1975; Newman, 1979, 1980), experiments with glial-specific toxins (Szamier et al., 1981; Bonaventure et al., 1981; Welinder et al., 1982), an ontogenic study (Rager, 1979), tests of ERG sensitivity to external K<sup>+</sup> (Miller, 1973; Dowling and Ripps, 1976), latency comparisons of b-waves vs. activation of the retinal network (Niemeyer, 1975; Rager, 1979), and K<sup>+</sup>-selective microelectrode studies (Dick and Miller, 1978*a*; Kline et al., 1978). Our present results are also entirely consistent with the Müller cell theory. We have characterized a distal light-evoked K<sub>o</sub><sup>+</sup> increase that is well developed at the level of the OPL and whose sensitivity to pharmacological agents closely parallels that of the b-wave. This distal K<sub>o</sub><sup>+</sup> increase could give rise to depolarization of Müller cell processes in the outer retina. In contrast, the pharmacological properties of the proximal K<sub>o</sub><sup>+</sup> increase in mudpuppy do not support the idea that it plays a primary role in the initiation of the b-wave; it cannot, however, be excluded as a contributing factor. Consistent with this idea, every study that has compared the properties of the proximal K<sub>o</sub><sup>+</sup> increase and the b-wave has concluded that the proximal K<sub>o</sub><sup>+</sup> response cannot be a primary factor in b-wave generation (Oakley, 1975; Dick and Miller, 1978; Kline et al., 1978; Dick, 1979; Vogel and Green, 1979, 1980; Vogel, 1980). The reasons these largest K<sub>o</sub><sup>+</sup> increases do not dominate K<sup>+</sup>-mediated transglial current flows detected as transretinal electroretinographic components are likely to involve the way in which the extracellular resistive pathway and electrotonic properties of Müller cells influence such currents (Newman, 1980, 1981, 1984; Newman and Odette, 1982, 1984; Newman et al., 1984). Additionally, it is known that glia can participate in the maintenance of extracellular K<sup>+</sup> homeostasis through both spatial and electrochemical buffering mechanisms (Somjen, 1979; Coles and Tsacopoulos, 1979; Gardner-Medwin, 1983; Newman, 1984). It remains to be investigated whether Müller cells participate in K<sup>+</sup> redistribution and how such phenomena are related to light-evoked K<sub>o</sub><sup>+</sup> modulations and the ERG.

In summary, the present study supports the concept that the b-wave and slow PIII components of the I-type ERG are generated through K<sup>+</sup>-mediated influences in Müller cells. We have observed two sources of light-evoked K<sup>+</sup> release, in distal and proximal retina, which can be differentially manipulated with pharmacological agents. The pharmacological properties of the proximal light-evoked K<sub>o</sub><sup>+</sup> increase indicate that it is primarily post-bipolar in origin. The pharmacological properties of the distal light-evoked K<sub>o</sub><sup>+</sup> increase indicate that it is primarily, if not exclusively, of depolarizing bipolar cell origin. When we combine our findings with those of other ERG studies (Faber, 1969; Miller and Dowling, 1970*a, b*; Rager, 1979; Newman, 1979, 1980), the following model of b-wave generation is suggested. Light-evoked depolarization of the depolarizing bipolars gives rise to K<sup>+</sup> efflux in the outer retina. This K<sup>+</sup> efflux depolarizes Müller cell processes, initiating a transretinal current flow associated with the primary voltage of the b-wave of the ERG. Consequently, we suggest that the b-wave is primarily a second-order signal of depolarizing bipolar cell activity.

We thank Mrs. Rita Drochelman and Mrs. Linda Hammond for typing the manuscript and Ms. Judy Dodge for help with graphics.

This work was initiated and served as the basis of the doctoral thesis of E.D. in the Department of Physiology of the State University of New York at Buffalo. This work was supported in part by National Institutes of Health postdoctoral research fellowship EY07057 to E.D. and National Eye Institute grants EY00844 and EY02327 to R.F.M.

*Original version received 30 July 1981 and accepted version received 11 February 1985.*

#### REFERENCES

- Berger, S. J., M. L. McDaniel, J. C. Carter, and O. H. Lowry. 1977. Distribution of four potential transmitter amino acids in monkey retina. *J. Neurochem.* 28:159–163.
- Bonaventure, N., G. Roussel, and N. Wioland. 1981. Effects of DL- $\alpha$ -amino adipic acid on Müller cells in frog and chicken retinae in vivo: relation to ERG b-wave, ganglion cell discharge and tectal evoked potentials. *Neurosci. Lett.* 27:81–87.
- Brindley, G. S., and D. I. Hamasaki. 1963. The properties and nature of the R membrane of the frog's eye. *J. Physiol. (Lond.)*. 167:599–606.
- Brown, P. B., B. W. Maxfield, and H. Moraff. 1973. *Electronics for Neurobiologists*. MIT Press, Cambridge, MA. p. 394.
- Caldwell, J. H., N. W. Daw, and H. J. Wyatt. 1978. Effects of picrotoxin and strychnine on rabbit retinal ganglion cells: lateral interactions for cells with more complex receptive fields. *J. Physiol. (Lond.)*. 276:277–298.
- Cervetto, L., and M. Piccolino. 1974. Synaptic transmission between photoreceptors and horizontal cells in the turtle retina. *Science (Wash. DC)*. 183:417–418.
- Cohen, A. I. 1965. A possible cytological basis for the "R" membrane in the vertebrate eye. *Nature (Lond.)*. 205:1222–1223.
- Coles, J. A., and M. Tsacopoulos. 1979. Potassium activity in photoreceptors, glial cells and extracellular space in the drone retina: changes during photostimulation. *J. Physiol. (Lond.)*. 290:525–549.
- Dacheux, R. F., T. E. Frumkes, and R. F. Miller. 1979. Pathways and polarities of synaptic interactions in the inner retina of the mudpuppy. I. Synaptic blocking studies. *Brain Res.* 161:1–12.
- Dacheux, R. F., and R. F. Miller. 1976. Photoreceptor-bipolar cell transmission in the perfused retinal eyecup of the mudpuppy. *Science (Wash. DC)*. 191:963–964.
- Dick, E. 1979. Light- and dark-dependent extracellular K<sup>+</sup> activity modulations in the vertebrate retina: origins of electroretinographic components. Ph.D. Thesis. State University of New York, Buffalo, NY. 310 pp.
- Dick, E., and R. F. Miller. 1977. Extracellular potassium activity in the mudpuppy retina; its relationship to the b-wave of the ERG. *Soc. Neurosci. Abstr.* 3:557.
- Dick, E., and R. F. Miller. 1978a. Light-evoked potassium activity in mudpuppy retina: its relationship to the b-wave of the electroretinogram. *Brain Res.* 154:388–394.
- Dick, E., and R. F. Miller. 1978b. Contribution of K<sup>+</sup>-mediated Müller cell responses to ERG components of E- and I-type retinas. *Invest. Ophthalmol. Visual Sci.* 17(ARVO Suppl.):262. (Abstr.)
- Dick, E., R. F. Miller, and S. Bloomfield. 1985. Extracellular K<sup>+</sup> activity changes related to electroretinogram components. II. Rabbit (E-type) retinas. *J. Gen. Physiol.* 85:911–931.
- Dick, E., R. F. Miller, and R. F. Dacheux. 1979. Neuronal origin of b- and d-waves in the I-type ERG. *Invest. Ophthalmol. Visual Sci.* 18(ARVO Suppl.):34. (Abstr.)
- Dowling, J. E., and H. Ripps. 1976. Potassium and retinal sensitivity. *Brain Res.* 107:617–622.

- Faber, D. S. 1969. Analysis of the slow trans-retinal potentials in response to light. Ph.D. Thesis. State University of New York, Buffalo, NY. 303 pp.
- Frank, K., and M. C. Becker. 1964. Microelectrodes for recording and stimulation. *In* Physical Techniques in Biological Research. W. L. Nastuk, editor. Academic Press, Inc., New York. 5:22-87.
- Frank, K., M. G. F. Fuortes, and P. G. Nelson. 1959. Voltage clamp of motoneuron soma. *Science (Wash. DC)*. 130:38-39.
- Gardner-Medwin, A. R. 1983. A study of the mechanisms by which potassium moves through brain tissue in the rat. *J. Physiol. (Lond.)*. 335:353-374.
- Granit, R. 1935. Two types of retinas and their electrical responses to intermittent stimuli in light and dark adaptation. *J. Physiol. (Lond.)*. 85:421-438.
- Hagins, W. A., R. D. Penn, and S. Yoshikami. 1970. Dark current and photocurrent in retinal rods. *Biophys. J.* 10:380-413.
- Karwoski, C. J., M. H. Criswell, and L. M. Proenza. 1978. Laminar separation of light-evoked K<sup>+</sup> flux and field potentials in frog retina. *Invest. Ophthalmol. Visual Sci.* 17:678-682.
- Karwoski, C. J., C. Nicholson, and L. M. Proenza. 1982. K<sup>+</sup> sources in amphibian retina. *Soc. Neurosci. Abstr.* 8:50.
- Karwoski, C. J., and L. M. Proenza. 1977. Relationship between Müller cell responses, a local transretinal potential, and potassium flux. *J. Neurophysiol. (Bethesda)*. 40:244-259.
- Karwoski, C. J., and L. M. Proenza. 1978. Light-evoked changes in extracellular potassium concentration in mudpuppy retina. *Brain Res.* 142:515-530.
- Karwoski, C. J., and L. M. Proenza. 1980. Neurons, potassium, and glia in proximal retina of *Necturus*. *J. Gen. Physiol.* 75:141-162.
- Karwoski, C. J., and L. M. Proenza. 1982. Light-evoked K<sup>+</sup>-increases in amphibian retina. *Invest. Ophthalmol. Visual Sci.* 21(ARVO Suppl.):281. (Abstr.)
- Kennedy, A. J., M. J. Neal, and R. N. Lolley. 1977. The distribution of amino acids within the rat retina. *J. Neurochem.* 29:157-159.
- Kline, R. P., H. Ripps, and J. E. Dowling. 1978. Generation of b-wave currents in the skate retina. *Proc. Natl. Acad. Sci. USA.* 75:5727-5731.
- Lam, D. M. K. 1976. Synaptic chemistry of identified cells in the vertebrate retina. *Cold Spring Harbor Symp. Quant. Biol.* 40:571-579.
- Lam, D. M. K., and L. Steinman. 1971. The uptake of  $\gamma$ -<sup>3</sup>H aminobutyric acid in the goldfish retina. *Proc. Natl. Acad. Sci. USA.* 68:2777-2781.
- Lurie, M., and M. F. Marmor. 1980. Similarities between the c-wave and slow PIII in the rabbit eye. *Invest. Ophthalmol. Visual Sci.* 19:1113-1117.
- Martin, A. N., J. Swarbrick, and A. Cammarata. 1969. Physical Chemistry. Second edition. Lea and Febiger, Philadelphia, PA. 185-186.
- Matsuura, T., W. H. Miller and T. Tomita. 1978. Cone-specific c-wave in the turtle retina. *Vision Res.* 18:767-775.
- Miller, R. F. 1973. Role of K<sup>+</sup> in generation of b-wave of electroretinogram. *J. Neurophysiol. (Bethesda)*. 36:28-38.
- Miller, R. F., and R. F. Dacheux. 1976. Synaptic organization and ionic basis of on and off channels in mudpuppy retina. I. Intracellular analysis of chloride-sensitive electrogenic properties of receptors, horizontal cells, bipolar cells, and amacrine cells. *J. Gen. Physiol.* 67:639-659.
- Miller, R. F., R. F. Dacheux, and T. E. Frumkes. 1977. Amacrine cells in *Necturus* retina: evidence for independent  $\gamma$ -aminobutyric acid- and glycine-releasing neurons. *Science (Wash. DC)*. 198:748-750.

- Miller, R. F., and J. E. Dowling. 1970a. Intracellular responses of the Müller (glial) cells of mudpuppy retina: their relation to b-wave of the electroretinogram. *J. Neurophysiol. (Bethesda)*. 33:323–341.
- Miller, R. F., and J. E. Dowling. 1970b. A relationship between Müller cell slow potentials and the ERB b-wave. *Int. Soc. Clin. Electroretinography Symp. Pisa*. 85–100.
- Miller, R. F., T. E. Frumkes, M. Slaughter, and R. F. Dacheux. 1981a. The physiological and pharmacological basis of GABA and glycine action on neurons of the mudpuppy retina. I. Receptors, horizontal cells, bipolars and G-cells. *J. Neurophysiol. (Bethesda)*. 45:743–763.
- Miller, R. F., T. E. Frumkes, M. Slaughter, and R. F. Dacheux. 1981b. The physiological and pharmacological basis of GABA and glycine action on neurons of the mudpuppy retina. II. Amacrine and ganglion cells. *J. Neurophysiol. (Bethesda)*. 45:764–782.
- Newman, E. A. 1979. B-wave currents in the frog retina. *Vision Res.* 19:227–234.
- Newman, E. A. 1980. Current source-density analysis of the b-wave of frog retina. *J. Neurophysiol. (Bethesda)*. 43:1355–1366.
- Newman, E. A. 1981. Regional differences in retinal Müller cell membrane properties. *Soc. Neurosci. Abstr.* 7:275.
- Newman, E. A. 1984. Regional specialization of retinal glial membrane. *Nature (Lond.)*. 309:155–157.
- Newman, E. A., D. A. Frambach, and L. L. Odette. 1984. Control of extracellular potassium levels by retinal glial cell K<sup>+</sup> siphoning. *Science (Wash. DC)*. 225:1174–1175.
- Newman, E. R., and L. L. Odette. 1982. Model of electroretinogram b-wave generation: testing the K<sup>+</sup> hypothesis. *Soc. Neurosci. Abstr.* 8:50.
- Newman, E. A., and L. L. Odette. 1984. Model of electroretinogram b-wave generation: a test of K<sup>+</sup> hypothesis. *J. Neurophysiol. (Bethesda)*. 51:164–182.
- Niemeyer, G. 1975. The function of the retina in the perfused eye. *Doc. Ophthalmol.* 39:53–116.
- Noell, W. K. 1951. The effect of iodoacetate on the vertebrate retina. *J. Cell. Comp. Physiol.* 37:283–308.
- Noell, W. K. 1953. Studies on the electrophysiology and metabolism of the retina. Project No. 21-1201-004, Report No. 1. United States Air Force School of Aviation Medicine.
- Oakley, B. 1975. Measurement of light-induced transient changes in extracellular potassium ion concentration in the frog retina. Ph.D. Thesis. University of Michigan, Ann Arbor, MI. 173 pp.
- Oakley, B. 1977. Potassium and the photoreceptor-dependent pigment epithelial hyperpolarization. *J. Gen. Physiol.* 70:405–425.
- Oakley, B., D. G. Flaming, and K. T. Brown. 1979. Effects of the rod receptor potential upon retinal extracellular potassium concentration. *J. Gen. Physiol.* 74:713–737.
- Oakley, B., and D. G. Green. 1976. Correlation of light-induced changes in retinal extracellular potassium concentration with c-wave of the electroretinogram. *J. Neurophysiol. (Bethesda)*. 39:1117–1133.
- Penn, R. D., and W. A. Hagins. 1969. Signal transmission along retinal rods and the origin of the electroretinographic a-wave. *Nature (Lond.)*. 223:201–205.
- Proenza, L. M., and J. A. Freeman. 1975. Light-evoked extracellular potentials of the *Necturus* retina: current source density analysis of the electroretinographic b-wave and the proximal negative response. *Soc. Neurosci. Abstr.* 1:104.
- Rager, G. 1979. The cellular origin of the b-wave in the electroretinogram—a developmental approach. *J. Comp. Neurol.* 188:225–244.
- Schmidt, R., and R. Steinberg. 1971. Rod-dependent intracellular responses to light recorded

- from the pigment epithelium of cat retina. *J. Physiol. (Lond.)*. 217:71-91.
- Shimazaki, H., C. Karwoski, and L. Proenza. 1983. Pharmacological separation of Müller cells, (K<sup>+</sup>)<sub>o</sub> and the b-wave in mudpuppy retina. *Invest. Ophthalmol. Visual Sci.* 22(ARVO Suppl.):220. (Abstr.)
- Shimazaki, H., C. J. Karwoski, and L. M. Proenza. 1984. Aspartate-induced dissociation of proximal from distal retinal activity in the mudpuppy. *Vision Res.* 24:587-595.
- Somjen, G. G. 1979. Extracellular potassium in the mammalian central nervous system. *Annu. Rev. Physiol.* 41:159-177.
- Starr, M. S., and M. J. Voaden. 1972. The uptake of <sup>14</sup>Cγ-aminobutyric acid by the isolated retina of the rat. *Vision Res.* 12:549-557.
- Steinberg, R. 1971. Incremental responses to light recorded from pigment epithelial cells and horizontal cells of the cat retina. *J. Physiol. (Lond.)*. 217:93-110.
- Steinberg, R., and S. S. Miller. 1973. Aspects of electrolyte transport in frog pigment epithelium. *Exp. Eye Res.* 16:365-372.
- Steinberg, R. H., B. Oakley II, and G. Niemyer. 1980. Light-evoked changes in K<sub>o</sub><sup>+</sup> in the retina of the intact cat eye. *J. Neurophysiol. (Bethesda)*. 44:897-921.
- Steinberg, R., R. Schmidt, and K. T. Brown. 1970. Intracellular responses to light from cat pigment epithelium: origin of the electroretinogram c-wave. *Nature (Lond.)*. 227:728-730.
- Straschill, M., and J. Perwein. 1969. The inhibition of retinal ganglion cells by catecholamines and γ-aminobutyric acid. *Pflügers Arch. Eur. J. Physiol.* 342:45-54.
- Szamier, R. B., H. Ripps, and R. L. Chappell. 1981. Changes in the ERG b-wave and Müller cell structure induced by α-aminoadipic acid. *Neurosci. Lett.* 21:307-312.
- Tigges, J., B. A. Brooks, and M. R. Klee. 1967. ERG recordings of a primate pure cone retina (*Tupaia glis*). *Vision Res.* 7:553-563.
- Tomita, T. 1976. Electrophysiological studies of retinal cell function. *Invest. Ophthalmol. Visual Sci.* 15:171-187.
- Tomita, T., and A. Kaneko. 1965. An intracellular coaxial microelectrode—its construction and application. *Med. Electron. Biol. Eng.* 3:367-376.
- Vogel, D. A. 1980. Potassium release and ERG b-wave current flow in the frog retina. Ph.D. Thesis. University of Michigan, Ann Arbor, MI. 158 pp.
- Vogel, D. A., and D. G. Green. 1979. Potassium release and current flow in the frog retina: a test of the Müller cell hypothesis of electroretinogram (ERG) b-wave generation. *Soc. Neurosci. Abstr.* 5:813.
- Vogel, D. A., and D. G. Green. 1980. Potassium release and b-wave generation: a test of the Müller cell hypothesis. *Invest. Ophthalmol. Visual Sci.* 19(ARVO Suppl.):39. (Abstr.)
- Walker, J. L. 1971. Ion specific liquid ion exchanger microelectrodes. *Anal. Chem.* 43:89A-93A.
- Weakley, J. N. 1973. The action of cobalt ions on neuromuscular transmission in the frog. *J. Physiol. (Lond.)*. 234:597-612.
- Welinder, E., O. Textorius, and S. E. G. Nilsson. 1982. Effects of intravitreally injected DL-α-aminoadipic acid on the c-wave of the D.C.-recorded electroretinogram in albino rabbits. *Invest. Ophthalmol. Visual Sci.* 23:240-245.
- Witkovsky, P., F. E. Dudek, and H. Ripps. 1975. Slow PIII component of the carp electroretinogram. *J. Gen. Physiol.* 65:119-134.
- Yanagida, T., and T. Tomita. 1982. Local potassium concentration changes in the retina and the electroretinographic (ERG) b-wave. *Brain Res.* 237:479-483.
- Zuckerman, R. 1973. Ionic analysis of photoreceptor membrane currents. *J. Physiol. (Lond.)*. 235:333-354.